JOURNAL OF MATERIALS SCIENCE 17 (1982) 1221–1231

The effect of silicon on the structure and mechanical properties of an α + β titanium alloy

H. M. FLOWER, K. LIPSCOMBE, D. R. F. WEST
Department of Metallurgy and Materials Science, Imperial College of Science and Technology, London SW7 2BP, UK

Titanium 4 wt% Al–4 wt% Mo–2 wt% Sn containing 0, 0.25 and 0.5 wt% Si has been solution-treated in the α + β phase field at 900° C. The microstructures obtained at room temperature after cooling from 900° C at various rates have been determined using transmission electron microscopy and the partitioning of the elements between the phases has been established using X-ray energy dispersive analysis on the thin foils. The degree of partitioning increases with decreasing cooling rate: aluminium partitions to the α-phase, molybdenum and silicon to the β-phase and tin remains uniformly distributed. Silicon is found to inhibit the partitioning of molybdenum: this has a profound effect on the stability of the β-phase and the resultant microstructure. In quenched material containing transformed β, substantial age hardening can be obtained in the range 350 to 600° C and is associated with precipitation within the orthorhombic martensite phase, possibly occurring via a spinodal mechanism. Silicon has little effect on the microstructure of air-cooled samples but contributes to high-temperature strength via dynamic strain ageing.

1. Introduction

Silicon is introduced into titanium alloys to enhance their resistance to creep at elevated temperatures and a number of near α and α + β alloys incorporating silicon are currently available. The optimum level of silicon varies from alloy to alloy [1–4] but is generally limited to a maximum value only slightly in excess of the solid solubility limit at the homogenization or hot-working temperature. This ensures (a) that few coarse, and possibly deleterious, silicide particles are produced at this temperature and (b) that the amount of silicon in solution at the service temperature is maximized to inhibit creep through dynamic strain ageing [5, 6] or possibly by silicide precipitation on moving dislocations [7]. However, silicon affects not only the creep resistance but also the microstructure and static strength of titanium alloys [8, 9] and in alloys processed in the α + β phase field the partitioning of silicon, and the other alloying elements, between the phases must be considered in relation to property development. It is the purpose of the present work to examine the role of silicon in the development of the microchemistry, microstructure and static strength of an alloy base equivalent to that of a commercially available α + β titanium alloy IMI550.

2. Experimental procedure

The material used in this work was supplied by Imperial Metal Industries (Titanium) Ltd in the form of 19 mm diameter bar in lengths of approximately 5 m. The bar had been finished-rolled at 900° C in the α + β phase field. The compositions of the three alloys studied are given in Table I.

The standard commercial heat-treatment of IMI550 consists of a solution treatment at 900° C in the α + β phase field for 1 h per 25 mm of section thickness followed by air cooling and a stabilization anneal at 500° C for 24 h. This heat-treatment schedule was adopted for all mechanical test specimens but for microstructural studies both

0022–2461/82/041221–11$03.82/0

TABLE I Compositions of the alloys (wt%)

Alloy	Al	Mo	Sn	Si	O
0 wt% Si	4.11	3.80	2.09	0.03	0.235
0.25 wt% Si	4.02	3.73	2.08	0.22	0.205
0.5 wt% Si	3.93	3.71	2.07	0.50	0.228
IMI550 (nominal)	4	4	2	0.5	

water quenching and furnace cooling were also employed as variations after solution treatment. The effects of variation in treatment are also examined.

For the microstructural studies, 13 mm lengths of the bar stock were cut and heat treated in air at 900° C. After cooling, longitudinal sections of dimensions 8 mm x 8 mm x 1 mm were cut from the samples, ensuring that the surface layers were discarded, to provide specimens for hardness testing and light and electron microscopy. Ageing treatments in the range 350 to 600° C were carried out on these slices in sealed pyrex capsules containing high-purity argon. For the mechanical property studies 50 mm lengths of bar were heat treated at 900° C. After cooling, at least 1 mm was machined off all the bar surfaces and compression-test specimens 6 mm x 2.5 mm x 2.5 mm were cut from the bar, the major axis being parallel to the bar length. Again, all further heat treatments of these specimens were carried out in sealed argon-filled pyrex capsules. Compression testing was carried out at a strain rate of approximately $1.4 \times 10^{-4}\,\text{sec}^{-1}$. Strain rate sensitivity tests were carried out to investigate dynamic strain ageing. At least two specimens were tested at each selected temperature in the range 20 to 600° C. During the period of a given test the temperature variation was less than ± 2°. Preliminary results of this study are presented in [10].

Standard metallographic techniques were employed. Thin foils were examined in Phillips EM 301 and JEOL 120CX TEMSCAN electron microscopes. The latter microscope was equipped with a fully quantitative LINK X-ray energy dispersive microanalytical facility which was employed to determine the chemical compositions of the phases present in the thin foils.

3. Experimental results

3.1. Microstructure

The as-received structure of all three alloys was essentially similar and consisted of an approximately 3:2 mixture of α-grains and transformed β-grains which were elongated in the rolling direction (see Fig. 1a). After solution treatment at 900° C and air cooling, the grains were fully equiaxed but the rolling direction could still be determined via the connectivity between grains of the same phase (see Fig. 1b).

After water quenching from 900° C all three alloys appeared to be similar in the light microstructure with both α-grains and prior β-grains etching light (in aqueous solutions of 1% HF–12% HNO_3), except for the 0.5 wt% Si alloy for which a slight darkening of the β-phase was observed: this permitted evaluation of the α:β ratio at 1:1. Examination of thin foils by electron microscopy showed marked differences between the alloys with regard to the transformed β structure. In the silicon-free alloy (see Fig. 2a) the β-phase was almost completely retained with only a few martensite plates in some grains.

With increasing silicon content the amount of retained β decreased. Fig. 2b shows the 0.25 wt% Si alloy where areas of β can be seen between the martensite plates. These relatively large areas of retained β were not seen in the 0.5 wt% Si alloy but the larger change in amount of retained β occurred between the 0 and 0.25 wt% Si rather than between the 0.25 wt% and 0.5 wt% Si alloys. Where they occurred, the martensite plates contained stacking faults and twins in all three alloys. No ordering (or other reaction) was observed in the primary α-phase in any of the alloys, indicating that the Ti_3Al-phase was not formed during the solution-treatment procedure or subsequent quenching. In the 0.5 wt% silicon alloy, a very small number of coarse silicide particles were observed.

As with water quenching, light microscopy showed little difference between the alloys in the air-cooled condition. The equiaxed $\alpha + \beta$ nature of the alloys was apparent, with the transformed β-phase now etching dark as compared with the water quenched condition. This indicated a different transformation product in the β-phase. The volume-fraction of primary α was estimated to lie between 50 and 55 wt% for all three alloys.

Electron microscopy of the air-cooled samples showed the transformed β-regions to be the same in all the alloys. The structure consisted of plates of α, grown diffusionally to form a basket-weave structure (see Fig. 3). Layers of β were present between these α-plates, and were related to them crystallographically by the Burgers orientation

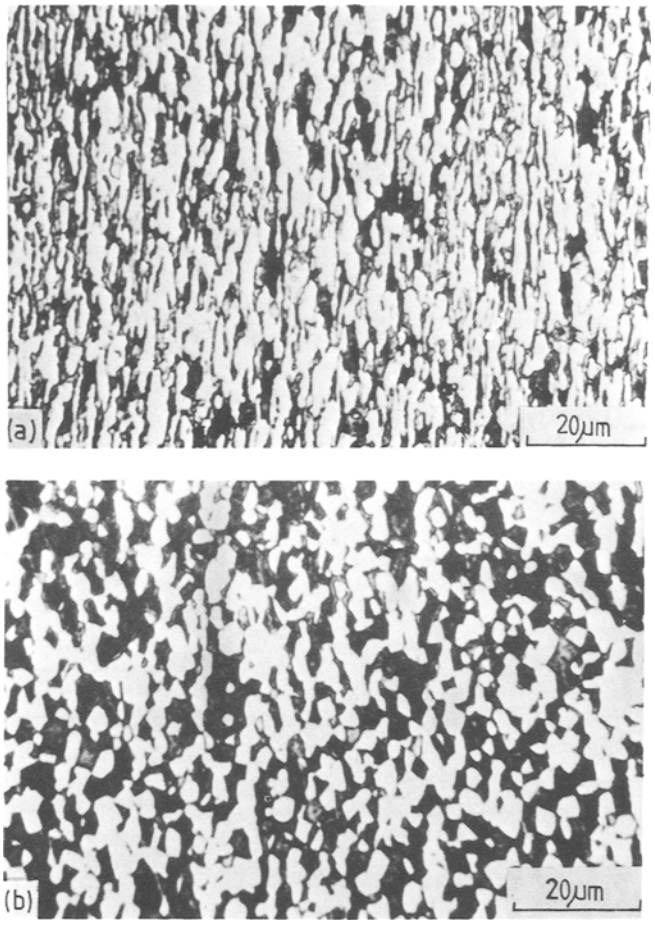

Figure 1 Longitudinal sections of the 0% Si alloy (a) in the as-received condition showing grains elongated in the rolling direction and (b) after solution treatment at 900° C and air cooling showing equiaxed grains with a high degree of connectivity between grains of the same phase in the rolling direction.

relationship. Selected-area diffraction patterns of the equiaxed α-grains exhibited only α reflections in all cases indicating that no ordering occurred within the α-phase.

After furnace cooling the percentage of α was significantly greater than in air- or water-cooled samples of all three alloys. Estimation of the relative amounts of α and β was carried out on thin-foil micrographs because the resolution of the etchant used in light microscopy was inadequate for accurate analysis of the minority β-phase. Monolithic interface α [11] was observed between the primary α- and β-phases and was included in the estimation of the α-phase: this was approxi-

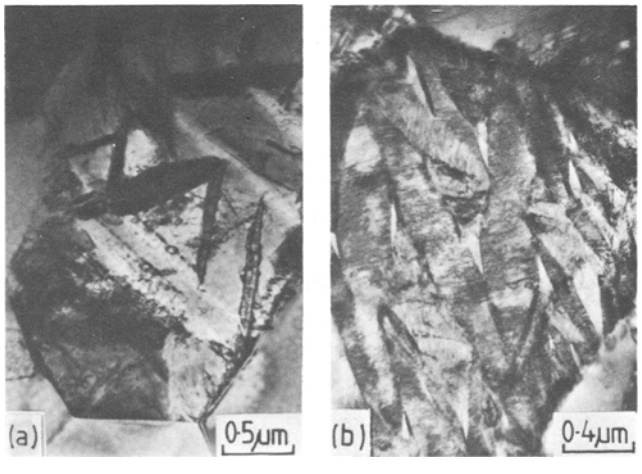

Figure 2 Electron micrographs of prior β grains after water quenching from 900° C. (a) 0% Si alloy showing only partial decomposition of the β-phase to martensite and (b) 0.25 wt% Si alloy showing almost complete transformation to martensite.

Figure 3 Electron micrograph of the 0% Si alloy after air cooling from 900° C. The microstructure consists of primary α-grains and prior β-grains which have been transformed on cooling to a basket-weave α + β structure.

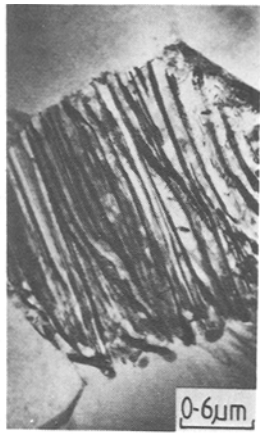

Figure 4 Electron micrograph showing the lamellar α + β structure produced in a prior β-grain in the water quenched 0% Si alloy upon ageing for 24 h at 500° C.

mately 80% in all three alloys. Limited selected-area diffraction studies were consistent with the expected face-centred cubic structure of the interface phase. The β-phase was retained at room temperature although selected-area diffraction indicated that some ω-phase was present in the silicon-free alloy. Again, no ordering was detected in the primary α-phase.

3.2. Microchemical analysis

The chemical compositions of the phases present in the 0 and 0.5 wt% Si alloys were determined using X-ray energy dispersive analysis in all three heat-treated conditions and in the water-quenched condition in the case of the 0.25 wt% Si material. In each case the electron microscope was used in the scanning transmission mode and as large an area as possible of constant thickness within the phase under investigation was scanned in order to obtain an accurate value of the phase composition. The foil thickness was determined from measurements of the parallax of either intersections of planar features with the foil surfaces or of deliberately-introduced surface contamination marks and used in the LINK analytical program for quantification of the raw X-ray data. The results are shown in Table II. The standard deviations shown are derived from at least ten analyses of different grains in each case. Spot analyses were also carried out to determine the composition of the interface α found in the furnace-cooled material. In all three cases the composition was close to that of the primary α but the measured molybdenum concentration tended to be higher (e.g., in the 0% Si alloy the interface α composition was 91.4 ± 0.3 wt% Ti, 4.0 ± 0.1 wt% Al, 2.4 ± 0.4 wt% Sn, 2.2 ± 0.5 wt% Mo). However, estimates of electron-beam broadening within the foil suggest that this may be due to excitation of X-rays from the adjacent molybdenum-rich β-phase.

3.3. Isochronal ageing treatments

The commercial 24 h ageing treatment at 500° C was carried out on samples of all three alloys in the water quenched, air and furnace cooled conditions. In the case of the water quenched material, light microcsopy revealed no change in the proportions of the phases present. Electron microscopy revealed that the β-phase of the 0% silicon alloy had decomposed by a cellular reaction to produce a lamellar α + β structure (Fig. 4). The martensite plates present to varying extents in all three alloys were seen to contain a very fine precipitate which was associated with a considerable increase in hardness (Table III). This precipitation reaction is considered in detail below. Ageing of air cooled samples had little discernable effect on the microstructure as determined by both light and electron microscopy, and hardness increased only slightly. The layers of β between the basket-weave α remained unspherodized. In the case of the 0.5 wt% silicon alloy some air cooled samples were further aged at 500° C for periods up to 170 h. Hardness decreased slightly from the peak value of 401 to 392. Microstructurally, the only change was in the β layers which were more

TABLE IIA Chemical compositions (wt%) of the α- and β-phases of water quenched alloys

Alloy (wt% Si)	Phase	Water quenched				
		Ti	Al	Sn	Mo	Si
0	α	91.5 ± 1.1	5.6 ± 0.6	2.1 ± 0.7	0.8 ± 0.6	
0	β	87.0 ± 1.1	3.7 ± 0.6	1.8 ± 0.9	7.5 ± 0.8	
0.25	α	92.2 ± 0.6	4.8 ± 0.3	2.1 ± 0.6	0.6 ± 0.4	0.3 ± 0.2
0.25	β	87.0 ± 1.2	3.3 ± 0.6	2.0 ± 0.8	7.4 ± 0.8	0.3 ± 0.2
0.5	α	91.0 ± 1.7	4.4 ± 0.6	2.2 ± 0.3	1.8 ± 1.0	0.6 ± 0.2
0.5	β	87.8 ± 0.9	3.2 ± 0.4	2.5 ± 0.3	5.9 ± 0.7	0.6 ± 0.2

TABLE IIB Chemical compositions (wt%) of the α- and β-phases of air cooled alloys

Alloy (wt% Si)	Phase	Air cooled				
		Ti	Al	Sn	Mo	Si
0	α	92.1 ± 0.6	4.8 ± 0.3	2.3 ± 0.2	0.8 ± 0.3	
0	β	87.3 ± 1.3	3.1 ± 0.7	2.2 ± 1.1	7.4 ± 0.9	
0.25	α					
0.25	β					
0.5	α	92.3 ± 0.7	4.6 ± 1.0	2.0 ± 0.5	0.7 ± 0.4	0.4 ± 0.1
0.5	β	87.2 ± 0.8	3.4 ± 0.3	2.2 ± 0.5	6.6 ± 0.8	0.6 ± 0.1

TABLE IIC Chemical compositions (wt%) of the α- and β-phases of furnace cooled alloys

Alloy (wt% Si)	Phase	Furnace cooled				
		Ti	Al	Sn	Mo	Si
0	α	92.7 ± 0.8	4.7 ± 0.5	2.1 ± 0.5	0.5 ± 0.4	–
0	β	77.7 ± 2.3	1.5 ± 0.6	2.3 ± 0.9	18.5 ± 2.6	–
0.25	α					
0.25	β					
0.5	α	91.6 ± 0.6	5.0 ± 0.6	2.3 ± 0.6	0.5 ± 0.5	0.6 ± 0.2
0.5	β	79.7 ± 1.8	1.9 ± 0.5	2.8 ± 1.1	14.7 ± 2.3	0.9 ± 0.7

clearly defined, suggesting that additional β-phase had grown during ageing. In the case of furnace cooled material, ageing caused the precipitation of coarse α-plates within the retained β-grains (see Fig. 5) and negligible hardening. In all cases the primary α remained unaffected by ageing.

3.4. Isothermal ageing treatments

In view of the very large increase in hardness obtained upon ageing structures containing martensite, isothermal hardness curves were determined for the water quenched 0.5 wt% Si alloy in the range 350 to 600° C. The results are shown in Fig. 6. Substantial age hardening can occur even at relatively low ageing temperatures. The microstructures associated with ageing are shown in Fig. 7 and are similar to those observed in the aged martensite plates of the other two alloys. Only two precipitate variants are formed with habit planes orthogonal to the basal plane of the martensite. In the early stages of ageing the precipitate distribution is uniform and continuous up to high-

TABLE III Isochronal ageing characteristics (24 h 500° C): Vickers hardness values

Alloy Si content (wt%)	Water quenched		Air cooled		Furnace cooled	
	Unaged	Aged	Unaged	Aged	Unaged	Aged
0	316	360	362	370	330	331
0.25	317	422	353	371	328	322
0.5	337	472	376	401	340	361

Figure 5 Electron micrograph showing Widmanstatten α-plates precipitated in a prior β-grain in the furnace cooled 0.25 wt% Si alloy upon ageing for 24 h at 500° C.

angle interfaces. As ageing proceeds, the particle dispersion coarsens uniformly, retaining the periodic arrangement of precipitates. Equilibrium β-phase precipitates on the high-angle interfaces and precipitate-free zones are formed within the plates adjacent to these particles. This suggests that the periodic precipitate array is metastable with respect to the β-phase.

3.5. Compression testing of air cooled material

This section describes the results of compression testing on the three alloys in the air cooled condition at temperatures up to 600° C. Light microscopy showed that the 0% Si alloy contained a shear band running across the diameter of the bar. It was though that this might affect the test results: to determine this some compression specimens were cut containing the band and their room-temperature properties were compared with those of specimens not containing the band. The results are shown in Table IV. It is reasonable to deduce from these results that, at least at room temperature, the shear band feature had no significant effect on the 0.2% proof stress and did not influence the results of the main compression testing programme. It is also possible to deduce that no great difference arises from the radial position of the compression specimens cut from the bar.

Fig. 8 shows the variation in 0.2% proof stress with temperature for the three alloys. The two silicon-containing alloys showed very similar behaviour: the 0.25 wt% Si alloy was about 100 MN m^{-2} weaker than the 0.5 wt% Si alloy at all temperatures. Both alloys showed a plateau in the proof stress value in the range of approximately 380 to 460° C. Up to a temperature of about 250° C the 0% Si alloy showed the same strength as the 0.25 wt% Si alloy, but, above this temperature, the curves diverged with the 0% Si alloy continuing with a decrease in slope, rather than a plateau, at around 400° C.

Fig. 9 shows the results from strain-rate cycling tests. Each alloy had a minimum value of strain-rate sensitivity at around 400° C corresponding to the range of the plateau or region of decreased

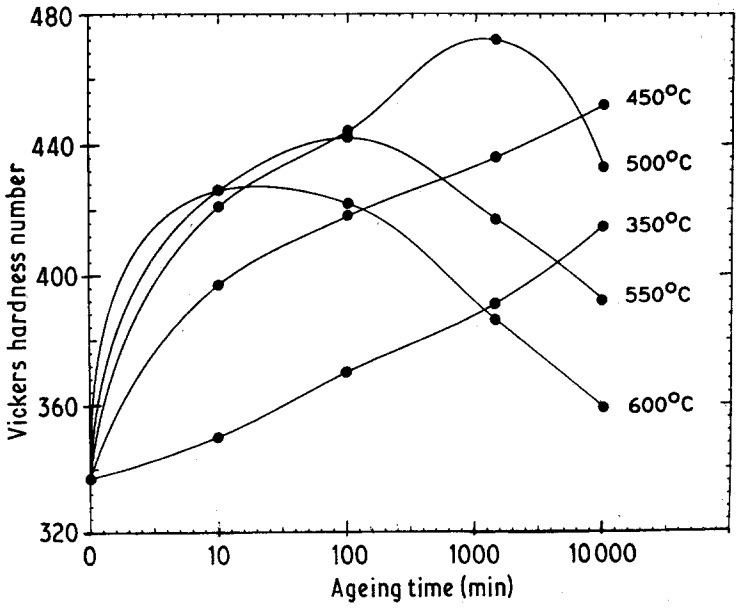

Figure 6 Age hardening curves for the 0.5 wt% Si alloy after solution treatment at 900° C (1h) followed by water quenching.

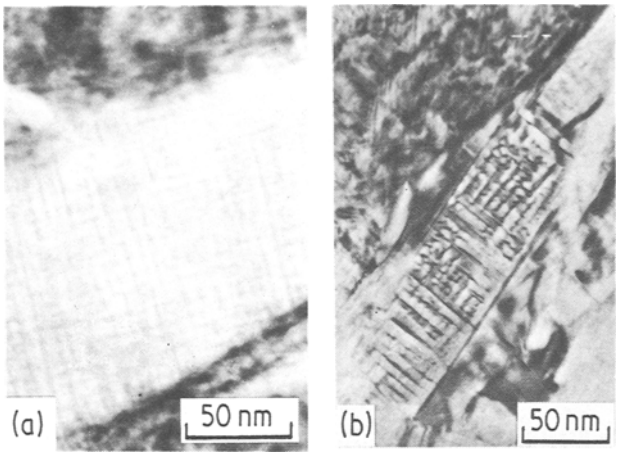

Figure 7 Electron micrographs showing precipitation within martensite plates of the water quenched 0.5 wt% Si alloy (a) after ageing for 24 h at 500° C and (b) after ageing for 100 min at 550° C. In both cases the martensite plates are shown close to the basal orientation in which the existance of only two precipitate variants can be clearly established.

slope in the proof stress measurements. Both silicon-containing alloys gave negative values in this region whereas the strain rate sensitivity always remained positive for the 0% Si alloys. Silicon appeared not only to affect the value of the minimum but also to move it to slightly higher temperatures (i.e., minimum values were found at approximately 405, 415 and 425° C for the 0, 0.25 and 0.5 wt% Si alloys, respectively).

4. Discussion

4.1. Solution heat-treatment and microstructure

The heat-treatment at 900° C produces approximately equal amounts of α- and β-phases in all three alloys. Chemical analysis of the water quenched samples indicates that aluminium partitions to the α-phase and molybdenum to the β-phase with tin and silicon being equally distributed between the phases. With the exception of silicon this behaviour is that expected of these elements. Silicon is a β-eutectoid forming element and might be expected to partition to the β-phase and to depress the $\beta \rightarrow \alpha$ transition on quenching. However, silicon does not affect the amounts of the phases present at 900° C and it was found experimentally that the amount of β retained, as β, on quenching decreases with increasing silicon content. The chemical analysis indicates that silicon actually decreases the partitioning of the molybdenum to the β-phase, and, hence, raises the Ms of the β-phase: it is believed that this is the reason for the decreased β-stability of the silicon-containing alloys. (The observation of a few silicide precipitates in the 0.5 wt% Si material indicates that the solubility limit at 900° C is slightly below this value.) The extent of partitioning increases with decreasing cooling rate. During cooling, the α-phase grows at the expense of the β-phase which becomes further enriched in molybdenum so that, on furnace cooling, the β-phase is sufficiently stabilized not to decompose diffusionally into α and β in all three alloys. Again the influence of silicon in inhibiting the partitioning of molybdenum is apparent and, although the scatter in the results is large, there is evidence of the expected partitioning of silicon to the β-phase. Since the ω-phase was observed only in the silicon-free alloy when the molybdenum content was greatest (and therefore when the ω-phase is less likely thermodynamically) it must be presumed that silicon also acts as an inhibiter of the ω-formation. Air cooling represents an intermediate case when partitioning during cooling is inadequate to prevent diffusional decomposition of the β-phase into the observed basket-weave $\alpha + \beta$ mixture. It is of interest to compare the present analytical results with those of Vaughan *et al.* [12] who analysed the phases present in commercial IMI550 after air cooling from several temperatures and then carrying out the stabilization anneal at 500° C. The comparison is shown in Table V. The ageing

TABLE IV Effect of shear band on room-temperature 0.2% proof stress of 0% Si alloy

Specimens containing shear band (MN m^{-2})	Specimens without shear band (MN m^{-2})
1035	1053
1041	1020
1053	1026
1035	1036
1035	1035
	1025
Mean = 1040 ± 8 MN m^{-2}	Mean = 1033 ± 12 MN m^{-2}

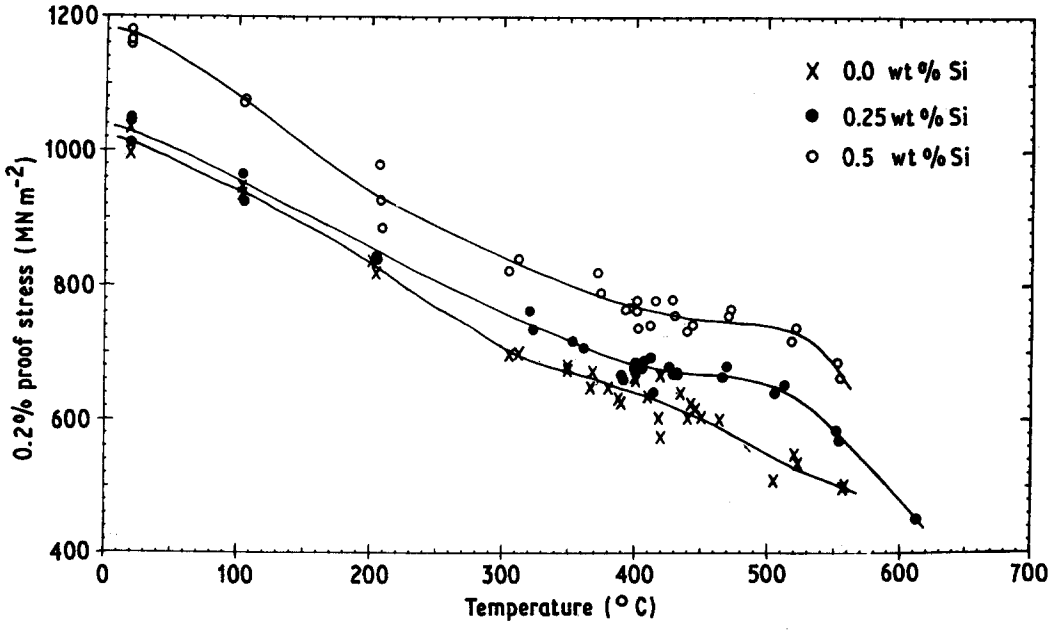

Figure 8 Variation of the 0.2% proof stress with temperature for all three alloys in the air cooled condition.

treatment at 500° C is most unlikely to have altered the extent of partitioning between primary α and β from that present after air cooling. The agreement between that work and the present analysis is, therefore, good and indicates that solution heat-treatment temperature and silicon content both significantly affect the extent of molybdenum partitioning. Again, in the work of Vaughan, silicon is seen to partition to the β-phase

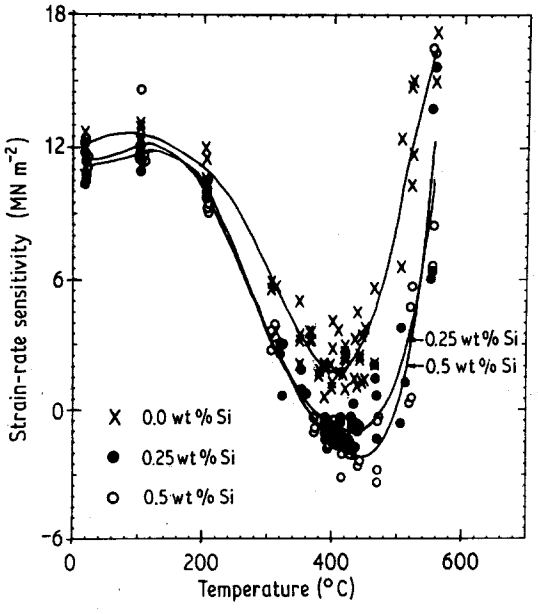

Figure 9 Variation of strain-rate sensitivity with temperature of all three alloys in the air cooled condition.

although the present work on water quenched material shows that this probably occurs during cooling and is not present at heat-treatment temperatures close to 900° C.

The interface α formed during slow cooling has been observed in many titanium alloys annealed in the $\alpha + \beta$ phase field and it is believed to be a cubic phase closely related to α. The chemical analysis in the present work shows a close similarity with that of α and is in agreement with recent results by Chenu *et al.* [13] on the interface α in slowly cooled IMI685 (Ti 6% Al 5% Zr 0.6% Mo 0.28% Si in that work). In common with the present work they observed a slightly higher molybdenum concentration in the interface phase but this could also be the result of pick-up of X-ray emission from the adjacent β-phase as suggested here.

Discussion of the hardness values of the three alloys must include consideration of the types and relative amounts of the phases present as well as of the degree of solution hardening present in the phases. It is clear that transformed β in the form of the basket-weave $\alpha + \beta$ produces more effective strengthening than an equivalent amount of martensite which produces little difference in hardness from retained β of similar composition. Silicon, in amounts up to 0.5 wt%, produces little hardening in any of the three heat-treated conditions, although its true effect may be masked by the fact that the silicon-free alloy has the highest oxygen content

TABLE V Composition of α- and β-phases as a function of heat-treatment temperature of IMI550 alloy

Alloy	Heat-treatment	Phase	Composition (wt%)				Reference
			Al	Sn	Mo	Si	
IMI550	875° C, air cooled and aged	α	4.12	1.95	1.40	0.39	[12]
		β (50%)	2.89	1.67	14.90	0.80	
0.5 wt% Si alloy	900° C, air cooled	α	4.6	2.0	0.7	0.4	Present
		β (50%)	3.4	2.2	6.6	0.6	work
IMI550	945° C, air cooled and aged	α	4.22	2.81	0.62	0.53	[12]
		β (75%)	3.81	2.53	6.02	0.68	
IMI550	960° C, air cooled and aged	α	4.60	2.13	0.86	0.52	[12]
		β (90%)	3.39	1.97	4.29	0.41	

and this element is a very potent solution-hardening agent.

4.2. Microstructural changes during ageing

The primary α-phase appears to be extremely stable and showed no tendency to order during any of the treatments to which the alloys were subjected. The retained β-phase decomposed via a cellular reaction in the case of the water quenched silicon-free alloy and via precipitation of α in the three furnace cooled alloys.

The difference in decomposition mode is indicative of the greater degree of metastability of the β-phase in the water quenched alloy as a consequence of its much lower molybdenum content compared with the furnace cooled material. Neither process would be expected to produce any substantial age hardening and this was observed in practice. It should be noted, however, that ageing of the β-phase at lower temperatures might produce precipitation of ω-phase and this could well result in considerable age hardening.

Ageing the air cooled material similarly resulted in little obvious change, although the absence of spherodization of the β-layers between the basket-weave α-plates of the transformed β-grains and the increased definition of these layers might suggest that more β is formed on holding at 500° C. There was no evidence of silicide precipitation indicating that the solubility limit for silicon is not exceeded at the ageing temperature.

The most significant microstructural and hardness changes were associated with the ageing of samples containing martensitic α. In all cases substantial increases in hardness accompanied the formation of the fine periodic precipitate dispersion within the martensite plates. The overall hardness change was least in the 0% silicon alloy since this contained the smallest volume-fraction of martensite: the cellular decomposition of the retained β-phase possibly provides some strengthening analogous to that observed in association with the transformed β-phase of the air cooled samples.

The precipitation within the martensite occurs with the formation of only two variants of particle. This suggests that the martensite is orthorhombic (α'') rather than hexagonal (α'). Sasano *et al.* [14] have studied the crystal structures of martensites in the Ti–Al–Mo system and, in the range of compositions observed here, they confirmed the presence of orthorhombic phase. Similar periodic precipitate arrays have been observed previously in binary-β isomorphous titanium alloys [15, 16] and were attributed to the spinodal decomposition within the orthorhombic martensite producing a metastable two-phase structure which subsequently transformed homogeneously (in the case of Ti–Mo) or heterogeneously (Ti–Nb) to equilibrium $\alpha + \beta$. Unpublished work by the same authors indicates that small (about 3 wt%) additions of aluminium do not alter the spinodal mechanism. It is therefore possible that the precipitation reaction observed here also represents a case of spinodal decomposition. Certainly, the initial absence of precipitate-free zones and their later development as heterogeneously nucleated β-phase begins to replace the periodic structure are consistent with the formation of a metastable two-phase structure via a spinodal mechanism.

4.3. Mechanical properties

The microstructural and ageing studies indicate that no significant structural changes can occur during the relatively short times of the elevated-temperature compression tests. The 0.2% proof stress values may therefore be taken to be those of equiaxed α plus transformed β observed in all the air cooled alloys. In any such multi-phase structure there will be a contribution to strength from the necessity for strain compatibility and slip trans-

fer across the interphase boundaries: evidence to that effect, has been obtained, for example, by Williams and Copley in two-phase Ti–6 wt% Al–4 wt% V [17]. In the present case, in all three alloys the volume-fractions of primary α and transformed β are similar, as are the grain sizes and microstructures of the transformed β. Therefore, differences in mechanical properties between the three alloys must be due to differences in alloying content. The higher proof stress of the 0.5 wt% Si alloy may be attributed to the solution strengthening produced by silicon. The smaller difference in proof stress between the 0.25 and 0 wt% Si alloys is consistent with the room-temperature hardness measurements and reflects the higher oxygen content of the latter alloy. The differences in strength are maintained to elevated temperatures and above about 400° C the strength of the silicon-free alloy falls relative to the others as a result of the formation of plateaux in the stress–temperature curves of these silicon-containing materials. Plateaux or peaks have been associated with dynamic strain ageing (DSA) in titanium alloys. Interstitials (O, N or C) can cause DSA in the range of approximately 280 to 530° C [18, 19] and it has been shown that the presence of misfitting substitutional solute atoms can increase the strength of the DSA via the formation of substitutional–interstitial atom pairs which, because of their non-spherically symmetrical strain fields, interact strongly with both edge and screw dislocations. Both silicon [20] and aluminium [21] have been cited in this regard. In the present case the DSA in the 0% Si alloy is insufficient to cause a distinct plateau but when silicon is present the effect is enhanced giving rise to plateaux extending up to about 500° C. The strain-rate sensitivity data are consistent with this interpretation. All the alloys show minima just above 400° C which correspond to the range of the plateau (or decreased slope in the case of the 0% Si alloy) in the proof stress curves. The negative values of strain-rate sensitivity observed in the alloys containing silicon indicate stronger pinning of dislocations compared to that due to oxygen alone. The fact that silicon slightly increases the temperature of the maximum DSA effect, as judged by both the plateau range and minima in the strain-rate sensitivity data, differs from the observations of Winstone *et al.* [20] who found that silicon lowered the temperature of DSA. However, the present results agree well with those obtained by Assadi *et al.* [9] in near-α alloys of composition close to that of IMI685 who found that silicon increased the temperature range of the DSA. The major difference between the present work and that of Assadi *et al.* lies in the microstructure. IMI685 is heat-treated in the β-phase field and is oil quenched. Thus, the entire microstructure consists of transformed β whereas, in the present work, some 50 to 55% is primary α. There is evidence in the present work of slight partitioning of silicon to the β-phase on air cooling but it is unclear what influence this has on the overall DSA effect. Creep resistance in titanium alloys containing silicon is attributed to DSA [5, 6] or to silicide precipitation on moving dislocations [7] and so more extreme silicon partitioning resulting from substantially slower cooling rates than those examined here could have very deleterious effects on creep resistance.

5. Conclusions

The microstructure of Ti–4 wt% Al–4 wt% Mo–2 wt% Sn is not significantly affected by the presence of silicon in the range 0 to 0.5 wt% at the solution heat-treatment temperature of 900° C. At this temperature aluminium partitions to the α-phase and molybdenum partitions to the β-phase. Air cooled microstructures are similar to one another regardless of silicon content in this range. Correspondingly, all three furnace cooled structures are similar to one another. Slight further partitioning of aluminium and molybdenum occurs during air cooling and considerable partitioning of molybdenum occurs during furnace cooling. Both at 900° C and during cooling, silicon inhibits the partitioning of molybdenum. There is also evidence of silicon partitioning to the β-phase during cooling.

On water quenching the silicon-free alloy from 900° C the β-phase is largely retained at room temperature with only a very small amount of martensite formation. Silicon lowers the molybdenum content of the β-phase at 900° C and consequently, on quenching, the β transforms further to orthorhombic martensite in the 0.25 wt% Si alloy and transforms completely in the 0.5 wt% Si material.

Ageing at 500° C produces little strengthening in air cooled or furnace cooled alloys. No significant microstructural changes were detected in the air cooled alloys and in the furnace cooled material α-phase plates precipitated in the β-phase. Ageing the orthorhombic martensite of quenched samples

in the range 350 to 600° C results in substantial age hardening due to precipitation in the martensite. This may occur via a spinodal decomposition mechanism.

The high-temperature strength of air cooled material is attributable to dynamic strain ageing by silicon in association with interstitial solute atoms.

Acknowledgements

The authors wish to thank Professor D. W. Pashley for the provision of laboratory facilities. The receipt of an SRC studentship by one of the authors (KL) is acknowledged. The project was supported under the SRC CASE scheme by the National Gas Turbine Establishment at Pyestock.

References

1. S. R. SEAGLE and H. B. BOMBERGER, "The Science, Technology and Application of Titanium" (Pergamon Press, Oxford, 1970) p. 1001.
2. G. S. HALL, S. R. SEAGLE and H. B. BOMBERGER, "Titanium, Science and Technology" (Plenum Press, New York, 1973) p. 3141.
3. C. E. SHAMBLEN and T. K. REDDEN, *Met. Trans.* **3** (1972) 1299.
4. S. R. SEAGLE, G. S. HALL and H. B. BOMBERGER, *Met. Trans. Quart.* Feb. (1975) 48.
5. M. R. WINSTONE, R. D. RAWLINGS and D. R. F. WEST, *J. Less Common Metals* **39** (1975) 205.
6. T. D. K. ASSADI, H. M. FLOWER and D. R. F. WEST, *Met. Tech.* **6** (1979) 16.
7. N. E. PATON and M. W. MAHONEY, *Met. Trans.* **A7** (1976) 1685.
8. H. M. FLOWER, P. R. SWANN and D. R. F. WEST, *J. Mater. Sci.* 7 (1972) 929.
9. T. D. K. ASSADI, H. M. FLOWER and D. R. F. WEST, *Met. Tech.* **1** (1979) 8.
10. K. LIPSCOMBE, H. M. FLOWER and D. R. F. WEST, Proceedings of the 5th International Conference on the Strength of Metals, Aachen, Vol. 1, edited by P. Haasen, V. Gerold and G. Kostorz (Pergamon Press, Oxford, 1979) p. 457.
11. C. G. RHODES and J. C. WILLIAMS, *Met. Trans.* **A6** (1975) 1670.
12. R. F. VAUGHAN, P. A. BLENKINSOP and D. F. NEAL, Proceedings of the 3rd International Conference on Titanium, Moscow, 1976 (Plenum Press, New York, 1980).
13. F. CHENU, C. SERVANT, C. QUESNE and P. LACOMBE, "Titanium '80" Science and Technology Metals Society AIME, Vol. 1. (AIME 1981) p. 725.
14. H. SASANO, T. SUZUKI, O. NAKANO and H. KIMURA, "Titanium '80" Science and Technology Metals Society AIME, Vol. 1 (AIME, New York 1981) p. 717.
15. R. DAVIS, H. M. FLOWER and D. R. F. WEST. Proceedings of the 3rd International Conference on Titanium, Moscow, 1976 (Plenum Press, New York, 1980) p. 1703.
16. R. DAVIS, H. M. FLOWER and D. R. F. WEST. *Acta Met.* **27** (1979) 1041.
17. S. M. COPLEY and J. C. WILLIAMS, "Alloy and Microstructural Design" (Academic Press, New York, 1976) p. 3.
18. A. T. SANTHANAM and R. E. REED-HILL, *Met. Trans.* **A2** (1971) 2619.
19. A. M. GARDE, A. T. SANTHANAM and R. E. REED-HILL, *Acta Met.* **20** (1972) 215.
20. M. R. WINSTONE, R. D. RAWLINGS and D. R. F. WEST, *J. Less Common Met.* **31** (1973) 143.
21. P. L. HARRISON, M. R. WINSTONE and R. D. RAWLINGS, *ibid.* **42** (1975) 137.

Received 15 July
and accepted 22 September 1981